Phase Structure and Properties of Poly(ethylene terephthalate)/High-Density Polyethylene Based on Recycled Materials

Yong Lei,[1] Qinglin Wu,[1] Craig M. Clemons,[2] Weihong Guo[3]

[1]*School of Renewable Natural Resources, Louisiana State University Agricultural Center, Baton Rouge, Louisiana 70803*
[2]*Performance Engineered Composites, USDA Forest Service, Forest Products Laboratory, One Gifford Pinchot Drive, Madison, Wisconsin 53705-2398*
[3]*Polymer Alloy Laboratory, Department of Materials Science and Engineering, East China University of Science and Technology, Shanghai 200237, People's Republic of China*

Received 12 June 2008; accepted 9 November 2008
DOI 10.1002/app.30178
Published online 17 April 2009 in Wiley InterScience (www.interscience.wiley.com).

ABSTRACT: Blends based on recycled high density polyethylene (R-HDPE) and recycled poly(ethylene terephthalate) (R-PET) were made through reactive extrusion. The effects of maleated polyethylene (PE-*g*-MA), triblock copolymer of styrene and ethylene/butylene (SEBS), and 4,4′-methylenedi(phenyl isocyanate) (MDI) on blend properties were studied. The 2% PE-*g*-MA improved the compatibility of R-HDPE and R-PET in all blends toughened by SEBS. For the R-HDPE/R-PET (70/30 w/w) blend toughened by SEBS, the dispersed PET domain size was significantly reduced with use of 2% PE-*g*-MA, and the impact strength of the resultant blend doubled. For blends with R-PET matrix, all strengths were improved by adding MDI through extending the PET molecular chains. The crystalline behaviors of R-HDPE and R-PET in one-phase rich systems influenced each other. The addition of PE-*g*-MA and SEBS consistently reduced the crystalline level (χ_c) of either the R-PET or the R-HDPE phase and lowered the crystallization peak temperature (T_c) of R-PET. Further addition of MDI did not influence R-HDPE crystallization behavior but lowered the χ_c of R-PET in R-PET rich blends. The thermal stability of R-HDPE/R-PET 70/30 and 50/50 (w/w) blends were improved by chain-extension when 0.5% MDI was added. © 2009 Wiley Periodicals, Inc. J Appl Polym Sci 113: 1710–1719, 2009

Key words: polyethylene; recycling; blends; poly(ethylene terephthalate)

INTRODUCTION

Plastics account for an increasing fraction of municipal solid waste around the world, and solid household waste is made up of a mixture of largely polyolefin-based resins, such as high-density polyethylene (HDPE), low-density polyethylene (LDPE), polypropylene (PP), Poly (ethylene terephthalate) (PET), etc. The plastic waste is not only polluting our waterways and seas, it is also beginning to take a toll on wildlife. Recycling plastic can reduce the resources needed in manufacturing, conserve energy in production and shipping, and minimize the overall impact on the environment over the life cycle of the product. PET and HDPE are used extensively in packaging materials, and their annual rates of growth of production and consumption steadily increase. Combining PET and PE can yield unusual properties. The blends can be less brittle than PET and may no longer need to be dried before processing. They are generally stiffer, better flowing, and faster cooling than HDPE, so they mold and extrude with faster cycles and higher outputs.[1] Thus, composite blends based on recycled PET (R-PET) and recycled HDPE (R-HDPE) have attracted increased interest.

Studies of PET/HDPE blends mainly focus on improving compatibility of PET and HDPE since they are inherently incompatible owing to the great difference in solubility parameters between them.[2] PET/HDPE blends have been compatibilized with elastomers [e.g., styrene-ethylene-butylenes-styrene block polymers (SEBS), ethylene-propylene rubber (EPR), and functionalized elastomers],[3–10] acrylic acid-based copolymers [e.g., ethylene-acrylic acid copolymers (E-AA), ethylene-glycidyl methacrylate copolymers (E-GMA), and ethylene-ethyl acrylate-glycidyl methacrylate terpolymers (E-EA-GMA)],[5–8,11–15]

Correspondence to: Y. Lei (yonglei168@hotmail.com) or Q. Wu (wuqing@lsu.edu).
Contract grant sponsor: United States Department of Agriculture Rural Development; contract grant number: 68-3A75-6-508.

functional group grafted polyolefins [e.g., polyethylene grafted with maleic anhydride (PE-*g*-MA), and polyethylene-*g*-isocyanate],[5,6,11,16–20] vinyl acetate-based copolymers,[21] and reactive monomers (e.g., silane and isocyanate).[3,22] For example, Coltelli et al. functionalized SEBS with diethyl maleate (DEM) or 2-hydroxyethyl methacrylate and added them to LDPE/R-PET (80/20) blends in the presence of $Ti(OBu)_4$ as transesterification catalyst.[4] The phase distribution depended strongly on composition, and, in particular, the preferential dispersion of R-PET in the SEBS-*g*-DEM was obtained when at least 40% by weight of LDPE was replaced by SEBS-*g*-DEM. Pracella et al.[5,6] compatibilized R-HDPE/R-PET (25/75) blends by melt-mixing in the presence of various functionalized polyolefins (e.g., HDPE-*g*-MA, EPR-*g*-MA, E-AA, E-GMA, and SEBS-*g*-MA). E-GMA was more effective than SEBS-*g*-MA in reducing the size of dispersed phase in R-PET and R-HDPE rich blends.[7] Pawlak et al. found that though the mechanical properties of R-PET rich blends were markedly improved by adding E-GMA, better performance was obtained with SEBS-*g*-MA in R-PE rich blends.[8] Carté et al. produced a PET/PE (50/50) blend containing 20 pph (part per hundred) SEBS-*g*-MA exhibiting a twofold increase in elongation at break relative to PE.[9] Functionalized polyolefins with reactive groups such as maleic anhydride, acrylic acid, and glycidyl methacrylate, can also effectively enhance the morphology and physical/mechanical properties of R-PET/R-HDPE blends.[16–20] However, all of these published studies on compatibilizing HDPE/PET blends were based on a limited compositional range, preventing an understanding of compatibilization over the full range of compositions. Also, a high loading of functional elastomer-based compatibilizer (e.g., 10–20 pph) was necessary to significantly improve toughness of the blends.[4–10,16,21]

Post-consumer PET undergoes a reduction in intrinsic viscosity or molar mass when recycled in a normal extrusion system because of thermal and hydrolytic degradation. This can result in significantly lower mechanical properties, especially tensile properties. Thus, reactive blending of PET with a chain extender, such as diphenyl carbonate, diphenyl oxalate, *bis*-2-oxazolines, *bis*-iminocarbonate, diisocyanate, and pyromellitic dianhydride (PMDA), were investigated to increase the lowered intrinsic viscosity during processing.[23–28] Both dianhydride and diisocyanate were addition-type chain extenders for polyesters.[24] PMDA was confirmed as an effective chain extender in the reactive extrusion of PET based on the rheological and thermal properties of PET.[25,26] Leistner et al.[27,28] used 4,4′-methylenedi (phenyl isocyanate) (MDI) as a chain extender for a carboxy-terminated poly(ethylene terephthalate-*co*-oxybenzoate), resulting a considerable increase in tensile strength, elastic modulus, and impact strength of the injection molded samples. However, very limited work has been done to study the effect of chain extenders on the properties of HDPE/PET blends.

In this work, a combination of an impact modifier (SEBS) and an interface compatibilizer (PE-*g*-MA) was used to modify R-HDPE/R-PET blends. A chain extender, diisocyanate, was also investigated as an additive. The objective of this research was to study the phase structure, crystallization behaviors, mechanical properties, and thermal stability of the formed blends over a wide range of R-HDPE/R-PET weight ratios.

EXPERIMENTAL

Materials

Typical recycled high-density polyethylene (R-HDPE) and recycled Poly (ethylene terephthalate) (R-PET) on the market were selected for the study. R-HDPE blocks and R-PET bottle scraps were obtained from Avangard Industries (Houston, TX). The melt flow index and density of R-HDPE were 0.7 g/10 min (190°C) and 939.9 kg/m^3, respectively. The block copolymer used was SEBS G1650M from KRATON Polymers U.S. LLC (Houston, TX) and had a polystyrene content of 30%. A maleated polyethylene (PE-*g*-MA) compatibilizer (Polybond® 3009) with a melt index of 5 g/10 min (190°C) and 1.00 wt % maleic anhydride was obtained from Chemtura Corporation (Middlebury, CT). The 4,4′-methylenedi(phenyl isocyanate) (MDI) was purchased from Aldrich Chemical Company (Saint Louis, MO). R-PET and PE-*g*-MA were dried in an oven for 10 h at 110°C before use.

Blend preparation

The raw materials were compounded in a 1-L thermokinetic high-shear mixer (i.e., K-mixer from Synergistics Industries) at 5000 rpm and discharged when a temperature of 215°C was reached. R-HDPE/R-PET weight ratios were 70/30, 50/50, and 30/70. The loading levels of MDI, PE-*g*-MA, and SEBS were 0.5%, 2%, and 5%, respectively, based on the total weight of R-PET and R-HDPE. Pure R-HDPE and R-PET blends were used as control.

The blends were granulated to pass a 1-cm screen, using a BP-68-SCS granulator (Sterling, New Berlin, WI). Specimens for mechanical testing were then injection-molded from the milled material using a 33-ton reciprocating-screw injection molder (Vista Sentry VSX, Milacron, Madison Heights, MI). The

specimens were molded at 310°C, with injection speed of 2.5 cm/s and a mold temperature of 49°C.

Characterization

Flexural and tensile properties were measured according to the ASTM D 790-03 and D 638-03, respectively, using an INSTRON machine (Model 1125, Boston, MA). For each blend, five replicates were tested. A TINIUS 92T impact tester (Testing Machine Company, Horsham, PA) was used for the Izod impact test. All samples were notched at the center point of one longitudinal side according to the ASTM D 256. For each treatment level, five replicates were tested.

FTIR analysis (Nicolet Nexus 670-FTIR, Thermo Electron Corporation, Gormley, Canada) on thin films of the plastics and their blends was made. The thin films were prepared by compression molding, using a two-sided stainless steel mold in a Wabash V200 hot press (Wabash, ID) under 30 tons of pressure. MDI was ground before use. Tests were run at a resolution of 2 cm^{-1}. A minimum of 150 scans were averaged.

The crystallization behaviors of R-HDPE and R-PET in the blends were measured using a differential scanning calorimeter (DSC Q100, TA Instruments, New Castle, DE). Samples of 4–5 mg were placed in aluminum capsules and heated from 40 to 270°C at 10°C/min and melt annealed for 5 min at 270°C to eliminate the heat history before cooling at 10°C/min. The crystallinity levels corresponding to the crystallization of HDPE and PET in blends were normalized to the mass unit of the specimens.

Thermogravimetric analysis (TGA) was employed to observe the thermal characteristics of the resultant blends on a Thermogravimetric Analyzer Q50 (TA Instruments) in a nitrogen environment at a scan rate of 10°C/min from room temperature to 650°C.

The morphologies of the blends were studied with a Hitachi VP-SEM S-3600N (Hitachi, Tokyo, Japan) scanning electron microscope. The samples were frozen in liquid nitrogen for 3 h and then quickly impact-fractured. The fracture surfaces of the specimens were sputter-coated with gold before analysis.

RESULTS AND DISCUSSION

Compatibilization and chain-extending reactions

Figure 1 shows the chemical interactions that presumably result from the chain extension reaction of the carboxyl or hydroxyl groups of R-PET with isocyanate groups of MDI and the reaction of the hydroxyl groups of R-PET with anhydride groups of

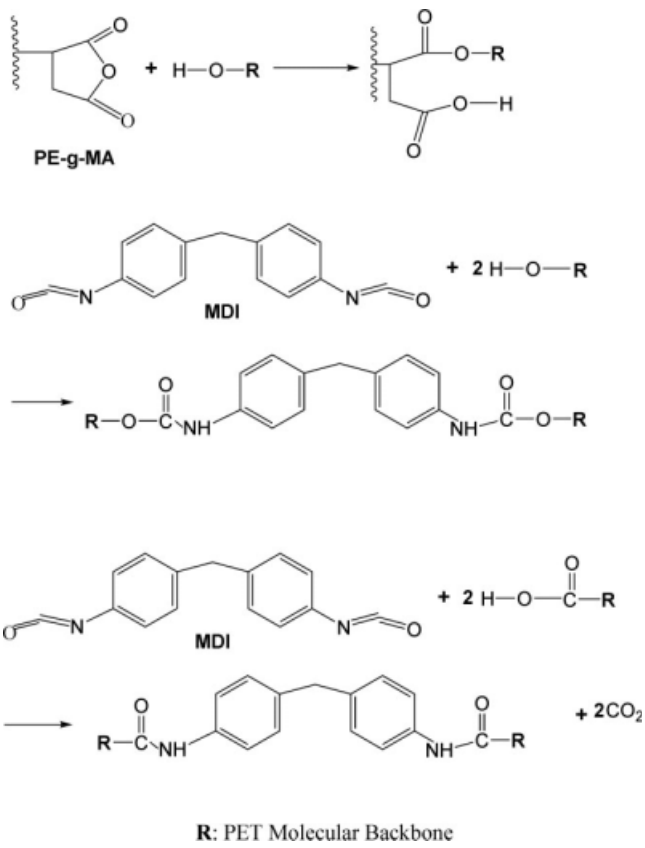

Figure 1 Main chemical reactions of the isocyanate groups of MDI or anhydride groups of PE-*g*-MA with R-PET.

PE-*g*-MA. Reactions between anhydrides and hydroxyl groups produce esters; the product of the isocyanate and hydroxyl group reaction is a urethane linkage, and reactions between the isocyanate and carboxyl group give rise to carbon oxide and amide linkages. Figure 2 shows the FTIR spectra of the raw materials and R-HDPE/R-PET (70/30 w/w) blends in the zone of 1500–3000 cm^{-1}. The interpretation of characteristic bands is presented in Table I.

The absorption peak at about 1791–1792 cm^{-1} (C=O stretching of anhydride) and 2270 cm^{-1} (N=C=O stretching) disappeared in the blends, indicating that the anhydride and isocyanate groups were completely reacted. The same behavior was found for the R-HDPE/R-PET blends at 50/50 w/w and 30/70 w/w ratios. The reaction between isocyanate groups of MDI with the functional groups of PET during extrusion was also confirmed by Leistner et al.[27,28] The anhydride groups of PE-*g*-MA were also observed to react with hydroxyl groups of PET during extrusion by other researchers.[17,19] The peak intensity at 1717 cm^{-1} (C=O stretching) in Figure 2 obviously increased when chain-extender, MDI, was introduced, possibly due to reactions between isocyanate and hydroxyl groups.

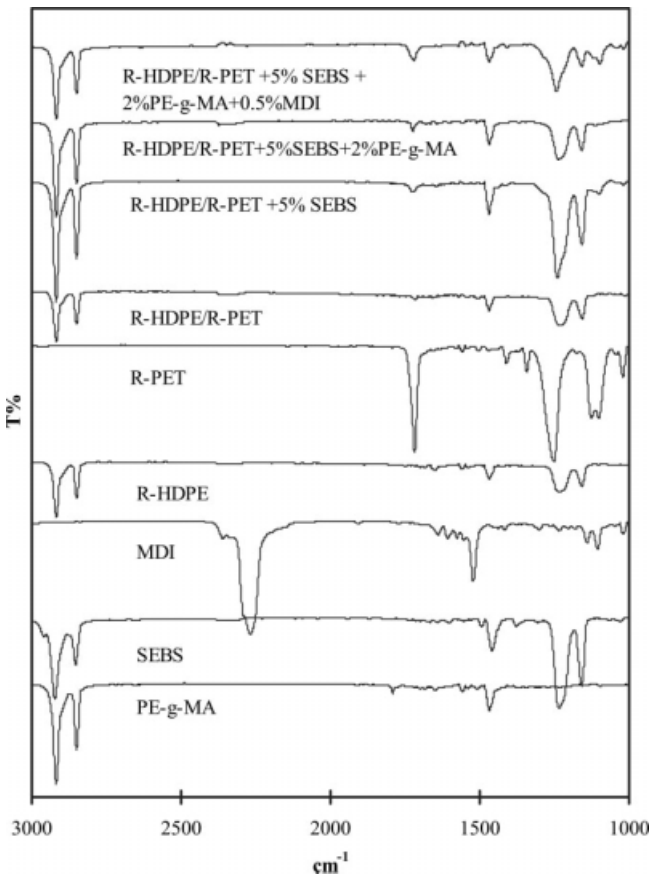

Figure 2 FTIR spectra of raw materials and R-HDPE/R-PET (70/30 wt %) blends.

Mechanical properties

Table II lists the mechanical properties of the blends. Except for the impact strength, the mechanical properties of R-PET were much higher than those of R-HDPE, especially the moduli. However, R-HDPE had more than twice the impact strength of the R-PET. For R-HDPE/R-PET binary blends without additives, flexural strength, flexural modulus, tensile strength, and tensile modulus were between those of neat R-HDPE and R-PET, increasing almost linearly with the increase of R-PET content. For impact strength, there existed minima, appearing when the blend contained 50 wt % R-HDPE and 50 wt % R-PET. The existence of the minimum mainly resulted from incompatibility between the R-HDPE and R-PET. The result agreed with those for virgin HDPE/PET blends obtained by Traugott et al.[10]

As shown in Table II, the addition of 5% SEBS increased the flexural and impact strengths of R-HDPE/R-PET (70/30) binary blends by about 10 and 40%, respectively, whereas other mechanical properties remained unchanged. Subsequent addition of the 2% PE-*g*-MA almost doubled the impact strength of the blend, which was 22.4% higher than that of neat R-HDPE, but lowered the tensile

TABLE I
FTIR Main Absorption Bands and Assignments of Bands from 1500 to 3000 cm^{-1}

Sample	Characteristic band (cm^{-1})	Interpretation
PE-*g*-MA	2,917, 2,849	CH stretching of CH_2
	1,791	C=O stretching
SEBS	2,922, 2,852	CH stretching of CH_2
MDI	2,270	N=C=O stretching
	1,608, 1,579, 1,521	Benzene skeletal vibration
R-HDPE	2,917, 2,849	CH stretching of CH_2
R-PET	1,717	C=O stretching
R-HDPE/ R-PET (70/30 w/w)	2,917, 2,849	CH stretching of CH_2
	1,718 (very weak)	C=O stretching
R-HDPE/R-PET (70/30 w/w) + additives	2,917, 2,849	CH stretching of CH_2
	1,718	C=O stretching

TABLE II
Effect of Additives on Mechanical Properties of R-HDPE/R-PET Blends[a]

R-HDPE/R-PET weight ratio	SEBS (%)	PE-*g*-MA (%)	MDI (%)	Flexural strength (MPa)	Flexural modulus (GPa)	Tensile strength (MPa)	Tensile modulus (GPa)	Impact strength (kJ/m^2)
100/0	–	–	–	27.1(0.7)	0.64(0.02)	26.0(0.1)	0.36(0.05)	13.35(0.69)
70/30	–	–	–	26.8(0.6)	0.79(0.04)	20.1(0.5)	0.89(0.09)	5.89(0.54)
	5	–	–	29.9(0.5)	0.84(0.08)	19.0(0.7)	0.81(0.05)	8.23(0.78)
	5	2	–	26.8(0.6)	0.68(0.04)	18.2(0.2)	0.59(0.11)	16.34(0.87)
	5	2	0.5	23.2(0.2)	0.70(0.06)	19.5(0.6)	0.90(0.07)	12.16(0.88)
50/50	–	–	–	38.7(0.7)	1.07(0.09)	3.7(0.6)	1.43(0.06)	2.10(0.07)
	5	2	–	34.3(0.6)	0.99(0.05)	22.5(0.2)	1.07(0.09)	3.07(0.07)
	5	2	0.5	35.5(0.7)	1.04(0.04)	23.4(0.7)	1.17(0.14)	3.67(0.11)
30/70	–	–	–	48.8(1.0)	1.57(0.05)	31.8(0.5)	1.09(0.10)	2.86(0.16)
	5	2	–	45.1(0.8)	1.41(0.06)	27.9(0.2)	1.20(0.12)	3.36(0.11)
	5	2	0.5	47.3(0.7)	1.42(0.08)	29.5(0.8)	1.12(0.05)	4.32(0.06)
0/100	–	–	–	83.3(1.0)	2.83(0.05)	50.4(0.5)	2.83(0.10)	3.89(0.24)

[a] The weight percentages of additives are based on the total weight of R-HDPE and R-PET.

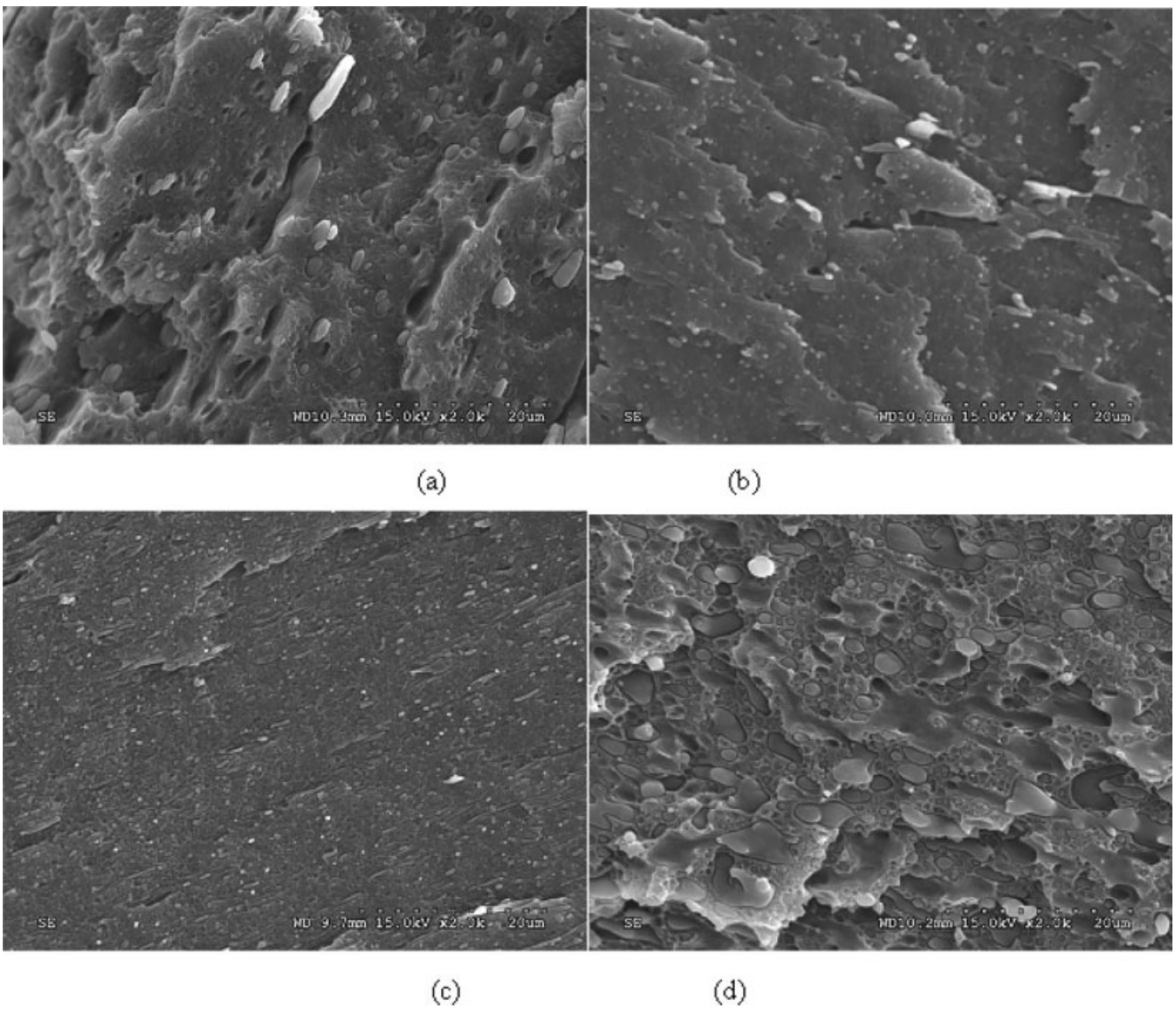

Figure 3 Morphology of the fracture surfaces of the R-PET/R-HDPE (30/70 w/w) blends with (a) no additives, (b) 5% SEBS and 2% PE-*g*-MA, (c) 5% SEBS, 2% PE-*g*-MA, and 0.5% MDI, and (d) 5% SEBS.

properties. Compared with the compatibilized and toughened R-HDPE/R-PET (70/30) blends, 0.5% MDI (i.e., the chain extender) reduced tensile and impact strengths, whereas tensile modulus was increased by about 53%.

For the R-HDPE/R-PET (50/50) binary blends, the addition of 5% SEBS and 2% PE-*g*-MA increased impact strength. The tensile and flexural strengths were lowered. All strengths were enhanced by subsequent addition of MDI, and the moduli remained at the same level. For the R-HDPE/R-PET (30/70) binary blends, the flexural and tensile strengths were lowered, the impact strength increased, but the moduli barely changed when PE-*g*-MA and SEBS were added. All strengths, especially the impact strength, were increased when MDI was subsequently added, and the moduli were hardly influenced.

Morphological characterization of the blends

Figures 3, 4, and 5 show the morphologies of the fracture surfaces of the R-HDPE/R-PET blends at different compositions. Without the compatibilizer, blends for all investigated compositions show the typical morphology of incompatible systems with a poor distribution of the components and no adhesion between matrix and dispersed phase, as shown in Figures 3(a), 4(a), and 5(a). For the blends with a continuous R-HDPE matrix (R-HDPE/R-PET 70/30), the dispersed PET phase mainly existed as oriented domains with a wide diameter distribution, due to the coalescence of the minor phase during the compounding. With an increase in R-PET content to 50%, a coarse co-continuous morphology formed [Fig. 4(a)], similar to that described by Traugott et al.[10] When the R-PET weight ratio was increased

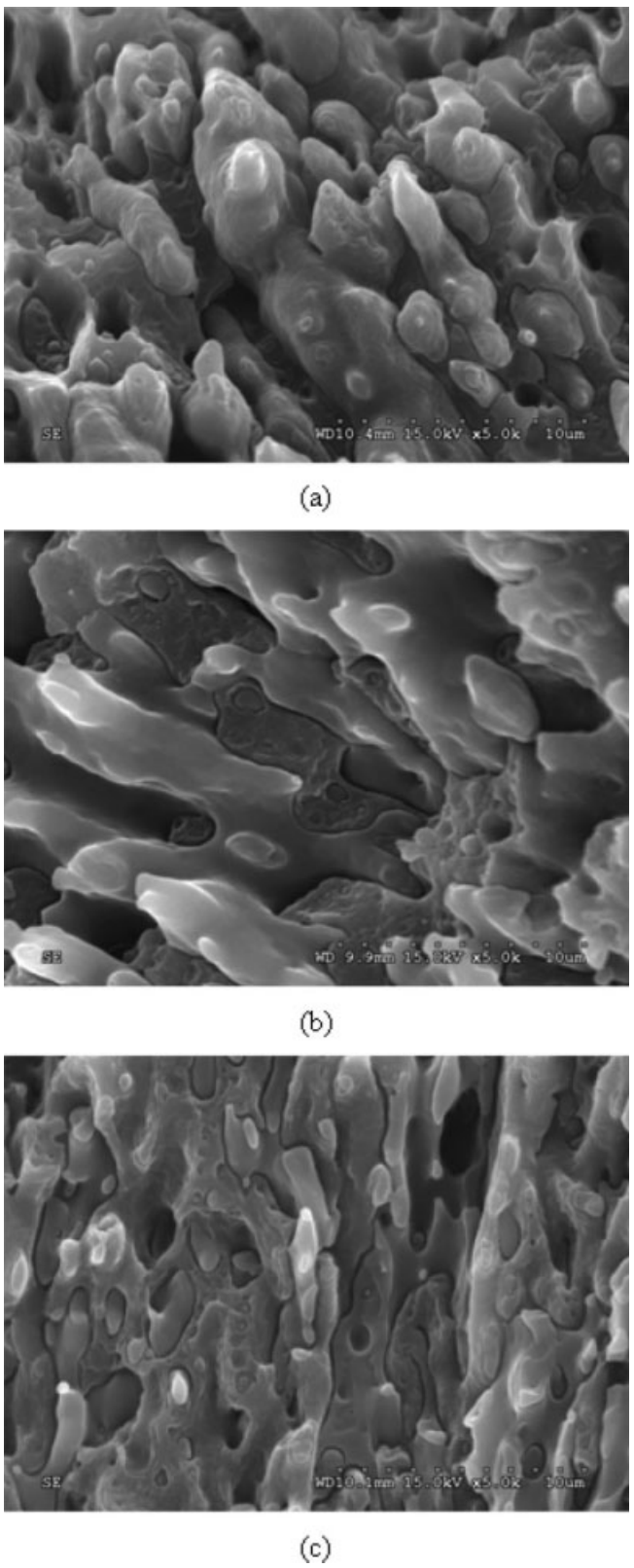

Figure 4 Morphology of the fracture surfaces of the R-PET/R-HDPE (50/50 w/w) blends with (a) no additives, (b) 5% SEBS and 2% PE-*g*-MA, and (c) 5% SEBS, 2% PE-*g*-MA, and 0.5% MDI.

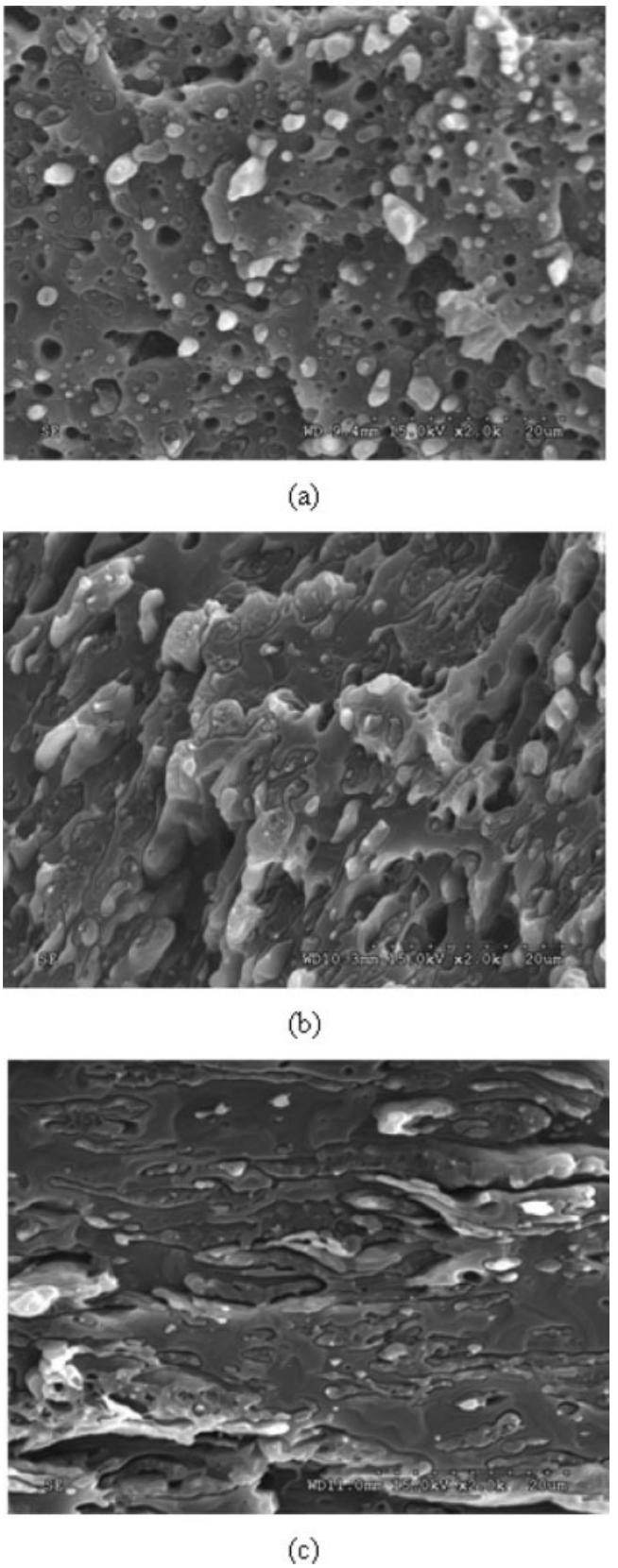

Figure 5 Morphology of the fracture surfaces of the R-PET/R-HDPE (70/30 w/w) blends with (a) no additives, (b) 5% SEBS and 2% PE-*g*-MA, and (c) 5% SEBS, 2% PE-*g*-MA, and 0.5% MDI.

to 70%, the HDPE phase became the dispersed phase with a wide diameter distribution [Fig. 5(a)]. There was no evidence of adhesion between the R-HDPE and R-PET phase since the phase interfaces were perfectly clear. Moreover, as shown in Figures 3(a) and 4(a), the voids occurring at places where the dispersed particles were located showed weak mechanical adherence between them.

When 5% SEBS was introduced, the R-HDPE/R-PET (70/30) blends displayed a larger average particle size of dispersed R-PET phase [Fig. 3(d)]. Thus, SEBS seemed to weaken the mechanical compatibility between R-PET and R-HDPE phases. The subsequent addition of PE-*g*-MA significantly reduced the R-PET particle size, most of which were less than 0.2 μm [Fig. 3(b)]. This reduction of dispersed particle size with the addition of compatibilizer is related to the decrease of interfacial tension and suppression of coalescence.[29] This suggests that the 2% PE-*g*-MA effectively improves the compatibility between R-PET and R-HDPE phases. The significant reduction of the dispersed PET phase and improved compatibility resulted in the significant improvement on the impact strength of the blends (Table II). The addition of MDI to the R-HDPE/R-PET (70/30) blends containing PE-*g*-MA and SEBS influenced the even dispersion and increased the average size of the dispersed R-PET phase, as shown in Figure 3(c), resulting in lowered tensile and impact strengths (Table II).

Adding PE-*g*-MA and SEBS appeared to reduce the R-HDPE phase size in the R-HDPE/R-PET (50/50) blends (Fig. 4), and the morphology became smooth. When MDI was subsequently added, there existed dispersed R-PET particles in the R-HDPE phase and dispersed R-HDPE particles in the R-PET phase, as shown in Figure 4(c). For the R-HDPE/R-PET (30/70) blends, the number of voids, which the dispersed particles left during fracture process, were significantly reduced by the compatibilizer [Fig. 5(b)]. The dispersed, irregular R-HDPE domains showed a wide diameter distribution and some clumpy R-HDPE domains, in which some small dispersed R-PET particles appeared. Further addition of MDI allowed forming a morphology shown in Figure 5(c). There still existed dispersed R-HDPE particles in the R-PET phase. At the same time, some small dispersed R-PET particles appeared in R-HDPE domains. The subphase morphology was previously found by other researchers in a similar PE/PET (50/50) blend.[9]

Crystallization behaviors

Figure 6(a) shows the DSC heating and cooling traces for pure R-HDPE and R-PET. At a heating rate of 10°C/min, a glass transition temperature of 73.7°C, a cold crystallization peak of 133.3°C, and a melting peak temperature of 251.4°C were found for R-PET. After melt annealing and cooling at 10°C/min, the crystallization peak temperature (T_c) found was 190.4°C. For R-HDPE, the melting peak and crystallization peak appeared at 133.9 and 112.0°C, respectively. The DSC cooling curves for pure R-HDPE, R-PET, and their uncompatibilized binary blends are shown in Figure 6(b). The T_c of R-HDPE was increased when R-HDPE was blended with R-PET, but the T_c of R-PET was decreased. The consistently increased T_c of R-HDPE in the binary blends suggests that the R-PET phase may nucleate the R-HDPE. The lowered bulk viscosity of the blends in the temperature range for PET crystallization by the molten R-HDPE probably resulted in the lowered T_c of R-PET.

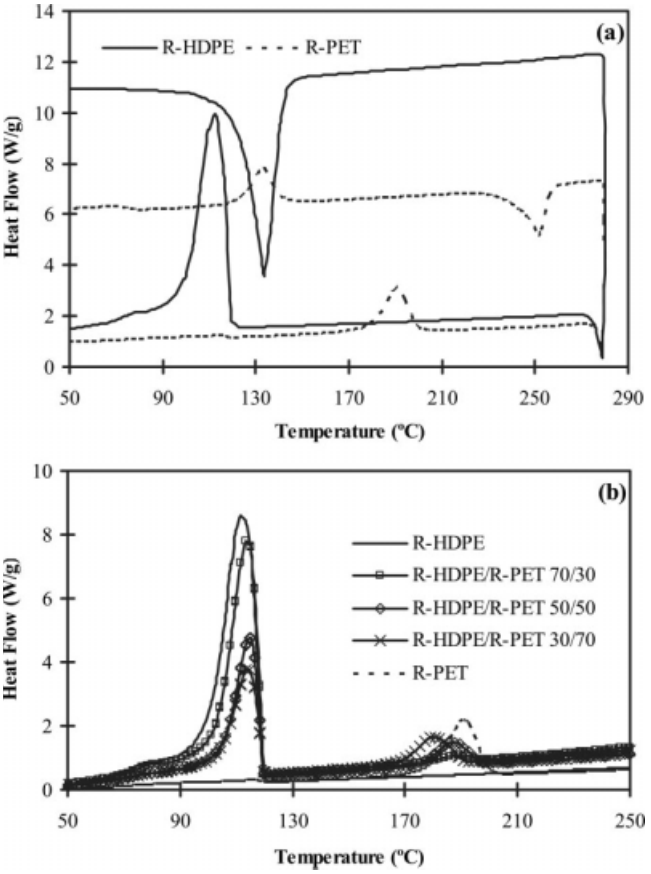

Figure 6 DSC heating and cooling curves for (a) pure R-HDPE and R-PET and (b) pure R-HDPE, R-PET, and their blends without additives. Heating and cooling rates of 10°C/min were used. Tests were performed in N_2 atmosphere.

The crystallinity level (χ_c) of R-HDPE and R-PET was evaluated from the following relationship:

$$\chi_c = \frac{\Delta H_{\text{exp}}}{\Delta H} \times \frac{1}{W_f} \times 100\%,$$

where ΔH_{exp} is the experimental heat of crystallization, ΔH is the assumed heat of crystallization of

TABLE III
Crystallization Behavior of HDPE and PET in R-HDPE/R-PET Blends[a]

R-HDPE/R-PET weight ratio	SEBS (%)	PE-*g*-MA (%)	MDI (%)	HDPE		PET	
				Peak temperature (°C)	χ_c (%)	Peak temperature (°C)	χ_c (%)
100/0	–	–	–	112.0	55.3	–	–
70/30	–	–	–	113.8	69.2	187.4	16.4
	5	–	–	113.4	62.7	178.6	11.4
	5	2	–	113.2	53.3	178.7	4.0
	5	2	0.5	115.1	52.5	179.1	3.8
50/50	–	–	–	114.4	51.5	186.0	25.5
	5	2	–	114.0	45.6	179.6	19.0
	5	2	0.5	114.7	44.9	175.3	13.2
30/70	–	–	–	114.0	66.3	185.5	19.2
	5	2	–	115.2	60.7	180.3	17.9
	5	2	0.5	115.5	50.8	180.0	15.5
0/100	–	–	–	–	–	190.4	26.8

[a] The weight percentages of additives are based on the total weight of R-HDPE and R-PET.

fully crystalline HDPE or PET, and W_f is the weight fraction of R-HDPE or R-PET in the blends. For fully crystalline HDPE, the heat of crystallization was assumed to be 276 J/g[30]; for fully crystalline PET, a value of 117 J/g was used.[31] The corresponding results are listed in Table III. The χ_c of R-HDPE was generally increased, and the χ_c of R-PET was decreased when the two plastics were blended without additives. The only exception to these trends was the R-HDPE/R-PET 50/50 (w/w) blend, in which the influence of blending on the χ_c on the blend components was minimal.

Adding compatibilizers consistently reduced χ_c of either PET or HDPE, with the largest changes occurring in the R-HDPE/R-PET (70/30). The χ_c reduction is indicative of the compatibility between components.[32] Adding MDI to the compatibilized blends further reduced the χ_c of both R-PET and R-HDPE phases, especially in blends with high R-PET content. For the R-HDPE phase, the influence of additives on the crystallization peak temperature was small. However, adding PE-*g*-MA and SEBS greatly lowered the T_c of R-PET phases in the blends. There was no further reduction in the T_c of R-PET when MDI was added, except for the R-HDPE/R-PET 50/50 (w/w) blend (Table III).

Thermogravimetric behaviors of the blends

Figure 7 shows the TGA weight loss traces of pure R-HDPE, R-PET, and their neat blends. The onset of decomposition temperature of R-HDPE was about 442°C, and the temperature at which R-HDPE degraded fastest was about 470°C. However, the R-PET began to degrade at about 387°C and degraded the fastest at about 425°C because of thermal and hydrolytic degradation.[26] The binary blends had two degradation peaks or shoulders, depending on the composition, resulting from R-PET and R-HDPE decomposition [Fig. 7(b)].

The decomposition shoulder of the neat R-HDPE/R-PET (30/70) binary blend merged into the main decomposition peak when PE-*g*-MA and SEBS were

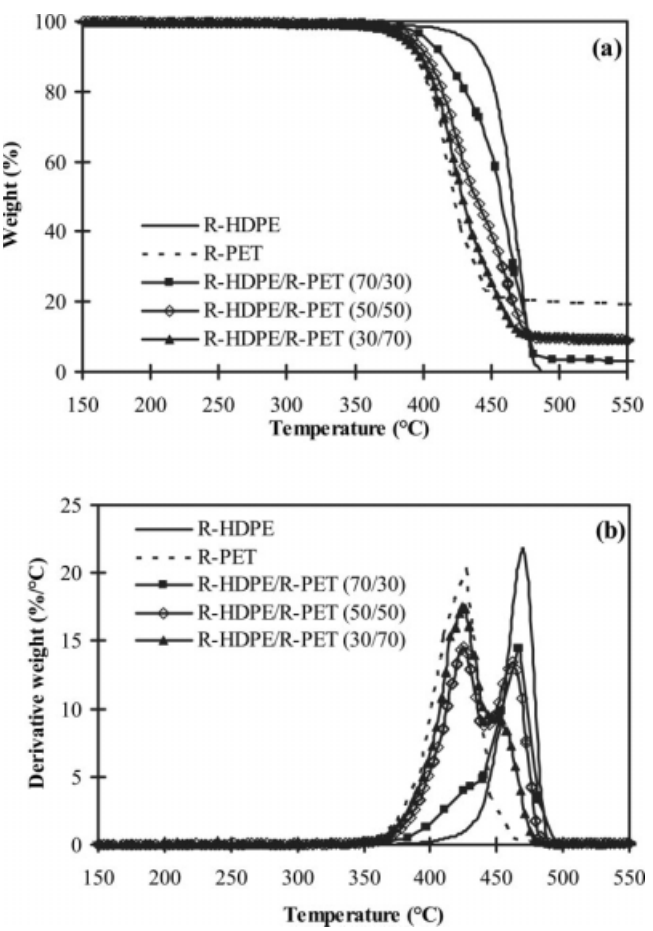

Figure 7 TGA curves of pure R-HDPE and R-PET and their neat binary blends at 10°C/min in N_2.

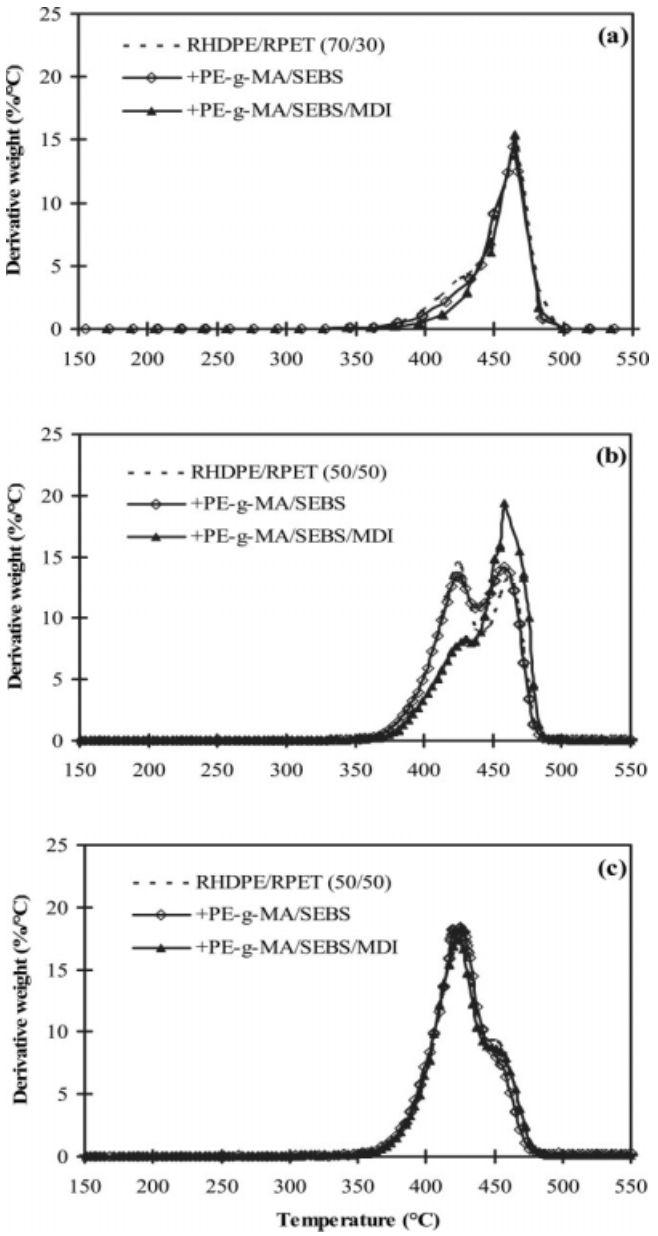

Figure 8 TGA curves of R-PET/R-HDPE blends with additives at 10°C/min in N_2.

added [Fig. 8(a)]. The subsequent addition of MDI to the blend further increased the onset of degradation temperature possibly because of improved thermal stability of the R-PET component after reacting with MDI. The enhanced R-PET thermal stability with addition of MDI is more apparent in the R-HDPE/R-PET (50/50) blend [Fig. 8(b)]. The addition of PE-*g*-MA and SEBS hardly affected the thermogravimetric behaviors of the R-HDPE/R-PET 50/50 and 30/70 (w/w) blends. Also, no obvious improvement in the thermal stability of the R-HDPE/R-PET 30/70 (w/w) blend was observed when 0.5% MDI was introduced [Fig. 8(c)].

CONCLUSIONS

The effects of impact modifier SEBS, compatibilizer PE-*g*-MA, and chain extender MDI on the reactive extrusion of blends of R-HDPE and R-PET were investigated. The morphologies and crystallization behaviors as well as the mechanical and thermal properties of the formed blends were studied.

In blends without any additives, the morphology was dependent on the relative weight ratios of the components, with the minor component existing as a dispersed phase in a matrix of the major component. For 50/50 w/w blends, the mechanical properties generally had some slightly negative deviation from additives, especially impact strength, presumably due to incompatibility. The crystallinity of R-HDPE was generally increased, but that of the R-PET was decreased when the two plastics were blended.

The use of additives influenced all properties measured for the blends. The R-HDPE/R-PET (70/30) was greatly affected by the additives at the levels used. Adding 2% PE-*g*-MA and 5% SEBS greatly influenced the R-PET domain size, suppressed R-HDPE and R-PET crystallinity, and improved impact performance. Subsequent addition of 0.5% MDI further influenced morphology and resulted in increase tensile modulus but lowered tensile and impact strengths. Further work will deal with blend performance optimized and their use in natural fiber reinforced composites. The blends provide potential matrix materials for natural fiber plastic composites.

This article is published with the approval of the director of the Louisiana Agricultural Experiment Station.

References

1. Akovali, G.; Bernardo, C. A.; Leidner, J.; Utracki, L. A.; Xanthos, M. Frontiers in the Science and Technology of Polymer Recycling; Kluwer Academic Publishers: Norwell, 1998.
2. Hansen, C. M. Hansen Solubility Parameters: A User's Handbook; CRC Press: Boca Raton, 2000.
3. Kratofil, L.; Hrnjak-Murgic, Z.; Jelencic, J.; Andricic, B.; Kovacic, T.; Merzel, V. Int Polym Proc 2006, 21, 328.
4. Coltelli, M. B.; Maggiore, I. D.; Savi, S.; Aglietto, M.; Ciardelli, F. Polym Degrad Stab 2005, 90, 211.
5. Pracella, M.; Rolla, L.; Chionna, D.; Galeski, A. Macromol Chem Phys 2002, 203, 1473.
6. Pracella, M.; Pazzagli, F.; Galeski, A. Polym Bull 2002, 48, 67.
7. Pluta, M.; Bartczak, Z.; Pawlak, A.; Galeski, A.; Pracella, M. J Appl Polym Sci 2001, 82, 1423.
8. Pawlak, A.; Morawiec, J.; Pazzagli, F.; Pracella, M.; Galeski, A. J Appl Polym Sci 2002, 86, 1473.
9. Carté, T. L.; Moet, A. J Appl Polym Sci 1993, 48, 611.
10. Traugott, T. D.; Barlow, J. W.; Paul, D. R. J Appl Polym Sci 1983, 28, 2947.
11. Choudhury, A.; Mukherjee, M.; Adhikari, B. Polym Polym Compos 2006, 14, 635.
12. Kaci, M.; Benhamida, A.; Cimmino, S.; Silvestre, C.; Carfagna, C. Macromol Mater Eng 2005, 290, 987.

13. Fasce, L.; Seltzer, R.; Frontini, P.; Pita, V. J. R.; Pacheco, E. B. A. V.; Dias, M. L. Polym Eng Sci 2005, 45, 354.
14. Morawiec, J.; Krasnikova, N. P.; Galeski, A.; Pracella, M. J Appl Polym Sci 2002, 86, 1486.
15. Guerrero, C.; Lozano, T.; González, V.; Arroyo, E. J Appl Polym Sci 2001, 82, 1382.
16. Pracella, M.; Chionna, D.; Ishak, R.; Galeski, A. Polym Plast Technol Eng 2004, 43, 1711.
17. Lusinchi, J. M.; Boutevin, B.; Torres, N.; Robin, J. J Appl Polym Sci 2001, 79, 874.
18. Kim, D. H.; Park, K. Y.; Kim, J. Y.; Suh, K. D. J Appl Polym Sci 2000, 78, 1017.
19. Sambaru, P.; Jabarin, S. A. Polym Eng Sci 1993, 33, 827.
20. Torres, N.; Robin, J. J.; Boutevin, B. J Appl Polym Sci 2001, 81, 2377.
21. Dimitrova, T. L.; La Mantia, F. P.; Pilati, F.; Toselli, M.; Valenza, A.; Visco, A. Polymer 2000, 41, 4817.
22. Demir, T.; Tincer, T. J Appl Polym Sci 2001, 79, 827.
23. Shima, T.; Urasaki, T.; Oka, I. Adv Chem Ser 1973, 128, 183.
24. Inata, H.; Matsumura, S. J Appl Polym Sci 1985, 30, 3325.
25. Incarnato, L.; Scarfato, P.; Maio, L. D.; Acierno, D. Polymer 2000, 41, 6825.
26. Awaja, F.; Daver, F. Polym Eng Sci 2004, 44, 1579.
27. Leistner, D.; Stephan, M.; Haussler, L.; Vogel, R.; Ratzsch, M. Angew Makromol Chem 1993, 206, 141.
28. Bohme, F.; Leistner, D.; Baier, A. Angew Makromol Chem 1995, 224, 167.
29. Lepers, J. C.; Favis, B. D.; Tabar, R. J. J Polym Sci Part B: Polym Phys 1997, 35, 2271.
30. Wunderlich, B.; Dole, M. J Polym Sci 1957, 24, 201.
31. Smith, C. W.; Dole, M. J Polym Sci 1956, 20, 37.
32. Utracki, L. A. Polymer Alloys and Blends: Thermodynamics and Rheology; Oxford University Press: New York, 1989.